Modeling, validation, exergy evaluation and optimization of an industrial cryogenic air distillation plant under variable demand

Camilo A. Mora, Alvaro Orjuela

Department of Chemical and Environmental Engineering,
Universidad Nacional de Colombia, 111321, Bogotá D.C., Colombia
camoramo@unal.edu.co; aorjuelal@unal.edu.co

Abstract. This study focused on the modeling, computer-aided simulation, validation, exergy evaluation and subsequent optimization of a thermally-integrated air separation facility. The model was implemented in HYSYS®, and it was assessed at the corresponding operating conditions of an existing air separation plant with a processing capacity of ~40 ton/h and without nitrogen demand. Reliability of the model was previously verified by making a comparison with data from the plant's manual at the base operating point and with historical records. The overall exergy efficiency was estimated in 0.18, and the specific power consumption (SPC) with respect to the produced oxygen in the plant was 1.26 kWh/Nm^3 O_2. Optimization of exergy and argon production was carried out considering the historical demand and the corresponding installed capacity of the plant. Exergy efficiency and argon recovery were enhanced up to 30% and 23%, respectively, by reducing the required feed flows with respect to manual recommendations.

Keywords Air separation, cryogenic distillation, exergy, optimization,

Introduction

Air separation is one of the most important processes at the industrial scale as air products are paramount in many different sectors (e.g, chemical, energy, electronics, food, heath services). Currently, air separation is mainly carried out by cryogenic distillation under high pressure, enabling to obtain high purity oxygen, nitrogen and argon. Because of the need for large compression and heat duties, cryogenic distillation is highly thermally integrated in order to reduce energy intensity of the system [1]. Typically, air distillation units are assessed with respect to the specific power consumption (SPC) per volume of oxygen at standard conditions, and nowadays, industrial plants operate with a SPC of around 0.3 kWh per Nm^3 O_2 [2]. Nevertheless, considering the large energy intensity of the process, there has been many attempts to optimize the cryogenic operation and to reduce energy consumption in order to improve sustainability indicators (i.e. economic, environmental, social) [3-7]. Considering that the air separation plants are highly thermally integrated, and that the available heat is generally below ambient temperature, optimization studies have been focused on reducing exergy destruction or losses to increase operating efficiency [8-13].

By mean of an exergy analysis it is possible to identify the equipment and sections of the plant that can be intervened to improve the overall efficiency [5]. In the particular case of air separation plants, it has been identified that multichannel heat exchangers, compressors and distillation columns, are the main source of exergy destruction and irreversibilities [9-11]. In this regard, the exergy analysis has enabled to identify highly efficient intensified schemes that can drive large efficiency improvements, such as peltlyuk configurations that replace traditional distillation columns [12], or thermal integrated processes within natural gas plants [13]. Nonetheless, optimization of air separations units depends on the local operating conditions as some plants are localized near to the client to cover a specific and variable demand. This demand can be mainly of oxygen and argon (highly valuable), while nitrogen is vented. In other facilities all the gases are valuable products and can be marketed. Besides, as the process operates under cryogenic condition, local ambient conditions play a key role in the efficiency of the process. Considering the particular conditions of each site, there is need for a specific exergy assessment of each particular plant.

In this context, the aim of this work was to carry out an exergy analysis of an existing cryogenic air distillation plant located in Colombia, in order to identify alternatives to improve efficiency under a current variable demand. As nitrogen is not marketed this stream is vented in this facility, and because the frequent shut-downs, the plant operates with a high specific power consumption of 1.26 kWh/Nm^3 O_2. Initially, a model of the existing air separation plant was implemented in Aspen HYSYS, using the corresponding equipment configurations, geometries, interconnections, and operating conditions. The model was validated by comparison of simulation results with data from the plant manual and also with historical records [14]. The exergy analysis enabled to identify the equipment with the lower efficiencies, and a subsequent sensitive analysis permitted to spot the key variables to optimize plant's performance. Finally, a multi-objective optimization was carried out to maximize exergy efficiency and argon recovery, under the currently variable monthly demand.

Methodology

Plant description and modeling

The studied air separation plant is described in Figure 1, and it includes an air purification section, compression, dehydration and a subsequent cryogenic conditioning and distillation. The last two sections constitute the so called "cold box" or cryogenic zone of the plant.

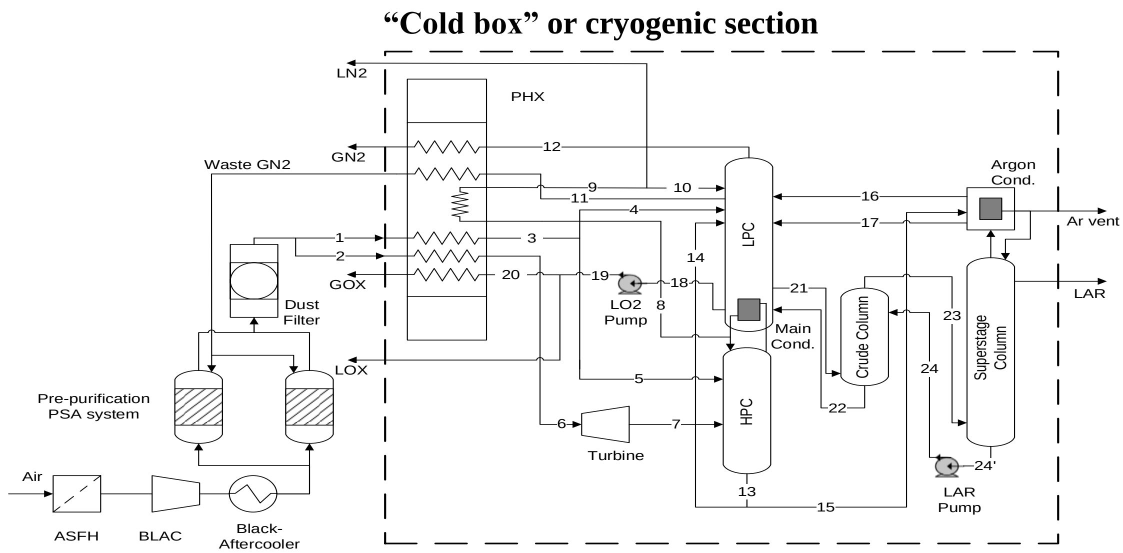

Fig. 1 Process flow diagram of the studied air separation unit and main operating variables

Initially, feed air passes through the filter (HASF) to removes dust particles before the multiple stage baseload air compressor (BLAC). The compressors increase air pressure from the local condition (0.74 bar) up to 50 bar. Afterwards the compressed stream is cooled down at ~ 20 ºC with water in a heat exchanger (BLAC-aftercooler). Subsequently, the air stream is treated to remove CO_2, water and hydrocarbons in a pressure swing adsorption (PSA) system. The adsorbed gases are later removed in the regeneration cycle using a waste nitrogen stream (Waste GN2) from the distillation units. Once purified, the air stream is fed to the cold box where it is divided in two streams (i.e. Lines 1 and 2) that are sent to the multichannel heat exchanger (PHX). Stream 2 is expanded, cooled and fed to the high-pressure column (HPC) to obtain high purity nitrogen stream at the top. This stream is thermally integrated with the reboiler of the low-pressure column (LPC). Stream 1 is subcooled and further divided in two streams (i.e. 4 and 5), one entering the HPC (5) to enhance separation and the other to the LPC to maintain argon recovery (4).

Nitrogen at the top of HCP is liquified by heat exchange with the boiling oxygen in the main condenser of the LPC. A portion of the liquified nitrogen is used as reflux for the LPC in the main condenser. The remaining fraction (8) is subcooled at the end of exchanger by heat transfer with the nitrogen gas streams (11 and 12) from the top of LPC; subsequently it is removed from the process as a product (GN2). The subcooled stream 9 is split into two streams (10 and LN2); the stream 10 is fed to the LPC at the top, and the stream LN2 is the liquid nitrogen product. The liquid from the HPC boiler (13) is divided into two streams (14 and 15); stream 14 is fed to the LPC and stream 15 is fed to the argon condenser at the top of the superstage column, where it boils by heat exchange with the condensing argon vapor. The resulting vapor stream (17) from this heat exchanger and a small amount of liquid (16) returns to the LPC. The products in the LPC are nitrogen gas (<2 ppm O2) at the top (12), liquid oxygen (> 99.6%) at the bottom (18), and residual nitrogen (11) withdrawn few stages from the top. Part of the compressed liquid oxygen (19) is removed as a product (LOX), and the rest (20) is boiled in the PHX by heat exchange with the condensing air under high pressure (1, 2). This last stream is heated close to ambient temperature (GOX).

Because of the large number of stages required in the argon-oxygen separation, it is necessary to divide the last column in a crude and superstage columns. The argon-rich vapor stream (21), containing 13.5% argon and less than 1 ppm nitrogen, is withdrawn from the bottom of the LPC and sent to the bottom of the crude column. The interconnection vapor and liquid streams between the crude and superstage columns are streams 23 and 24, respectively. The bottom stream of the crude column (22) is recycle to the LPC near the main condenser. Liquid argon is removed as a product (LAR) some stages below the top of the superstage column, and it contains < 2 ppm O2 and < 2 ppm N2. A small vapor purge is removed (Ar Vent) from the top of the column to prevent nitrogen accumulation. The complete process flow diagram of the process is presented in Figure 2 and the model was validated by comparison with data of the plant's manual and with historical records [14]. As observed multichannel heat exchanger was separated in sections to facilitate convergence and avoid temperature crossing. Also, to facilitate simulations and variables management, thermally-coupled distillation columns were divided and integration was done externally using heat exchangers. The crude and superstage columns in argon refining was assumed as a single unit. The corresponding process specifications are listed in Table 1.

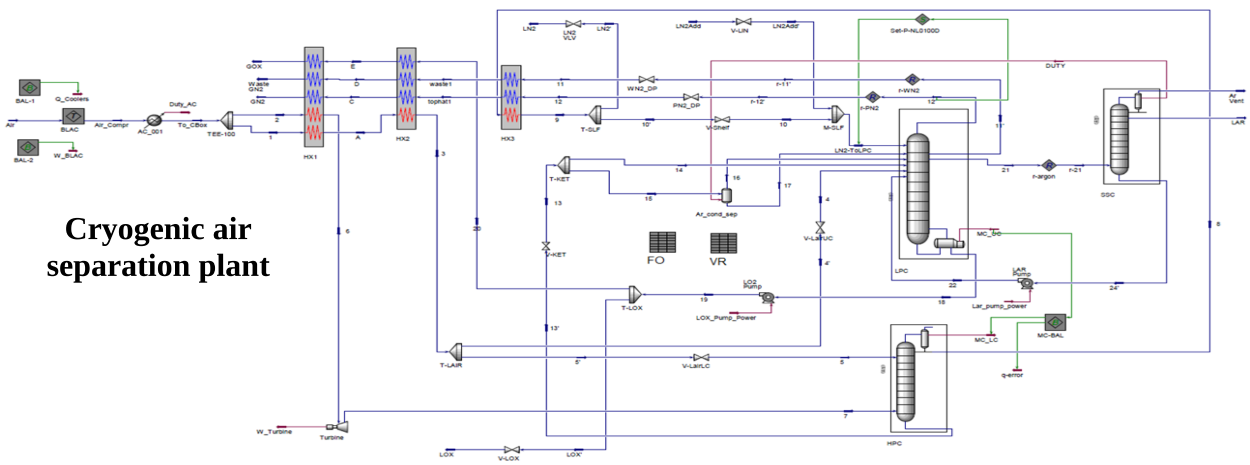

Fig. 2 Process flow diagram of the air separation plant as modeled in Aspen HYSYS

Table 1. Specification of the air separation plant at the base operational point (BOP)

Air feed conditions (equivalent to environment conditions)			Product requirements		
Variable		**Value**	**Stream**	**Concentration (% Mol)**	**Molar flow (kgmol/h)**
Molar flow rate (kgmol /h)		1.43	LN2	< 2 ppm O_2	0
Concentration (% mol)	N_2	78.12	LOX	> 99.6% O_2	
	O_2	20.95	LAR	< 2 ppm O_2	
	Ar	0.93		< 2 ppm N_2	
Temperature (K)		292.65	GOX	> 99.6% O_2	171.8
Pressure (kPa)		74			

Assessed process variables

All assessed variables were defined according with the current control scheme of the plant. A main operating variable is the inlet air flowrate, which defines cooling and operating capacity. Only a fraction of the total inlet air is required to provide the required cooling capacity of the plant, and this is set with variable X1 that defines the fraction of the inlet air that enters the turbine (stream 6) to be expanded at cryogenic temperatures. Optimization of X1 is required to ensure effective energy integration in the cold box, and to avoid either a large excess or a lack of cooling for a given operating capacity. The stream 3 from the multichannel heat exchanger is split into streams 4 and 5 to be fed at the (LPC) and (HPC), respectively. In this case, the manipulated variable (X2) was the split ratio of stream 3 that is fed to the HPC (i.e. flow of stream 5 with respect to stream 3). The main condenser is simulated as a thermal integration between the LPC reboiler and the HPC condenser. In this case, the variable ΔQ_C is the difference between the corresponding heat duties of the LPC reboiler (Q_{LPC}) and the HPC condenser (Q_{HPC}). X3 is fraction of nitrogen recovered in the top of LPC with respect to the total nitrogen fed to the process (nitrogen in air feed). X5 is the split ratio of liquid oxygen product (stream LOX) that is separated from stream 18. The liquid accumulated in the sump of the HPC (stream 13) is divided into two streams. One part is used as reflux of the LPC (stream 14) to provide enough cooling duty to withdraw as much oxygen as possible in the reboiler. The other part enables to provide enough flow in the argon condenser to remove the heat necessary to carry out the condensation (stream 15). In this case, the manipulated variable X4 is defined as the mass ratio of streams 14 with respect to stream 13.

Exergy evaluation
The exergy is a measure of the maximum theoretical work that can be obtained from a stream, from a mutual interaction with the environment until reaching equilibrium [5, 8]. However, the absolute values of the exergy destruction do not reflect the thermal efficiency, so it is necessary to use a rational exergy efficiency of Equation 1, defined as the ratio of the desired exergy output to the exergy used [8]. The desired exergy output ($\dot{E}_{desired\ output}$) is different for each equipment [8] and the corresponding equations of ε were reported in the literature [5]. $\dot{E}_D$ is the exergy destruction (irreversibilities) [15], and the calculation of physical and chemical exergies of material streams was done in Aspen HYSYS according to a reported method [16].

$$\varepsilon = \frac{\dot{E}_{desired\ output}}{\dot{E}_{desired\ output} - \dot{E}_D} \tag{1}$$

Optimization
The aim of the optimization is to maximize the rational exergy efficiency (ε) and argon recovery with respect to air feed flow (R_{LAR}); this is done considering a varying monthly demand in the studied plant. The objective function described in Equation 2 is subjected to operating variables (X_{opt}), process and thermodynamic constraints (X_{cons}), fixed specifications (X_{fix}), and the characteristic parameters of the industrial facility (X_{exp}). Problem formulation was similar to a previous report [17], but in this case a multi-objective optimization was performed.

$$\begin{aligned}
&\text{Objective Function: min } [-\varepsilon, -R_{LAR}]\\
&\text{subject to: } f\left(X_{prod}, X_{opt}, X_{fix}, X_{exp}, X_{cons}\right) = 0\\
&x_{prod} = [R_{LOX}, R_{LN2}]\\
&X_{cons}^L \le X_{cons} \le X_{cons}^U\\
&X_{opt}^L \le X_{opt} \le X_{opt}^U
\end{aligned} \tag{2}$$

The dimension and description of the different vectors are presented in Table 2, and some were fixed according to the specifications of the existing industrial plant. The vector of operating variables (X_{opt}) includes those to be manipulated in the optimization (Table 3), and their corresponding ranges were defined in a preliminary sensitivity analysis. Process constrains are summarized in Table 4, and optimization was done with a Nondominated Sorting Genetic Algorithm (NSGA-II) adopted from literature [18-20]. The algorithm was implemented in MatLab® interconnected with Aspen HYSYS®, and the problem was solved using a desktop computer that had an AMD Phenom 9550 Quad-Core 2.20 GHz processor and 8 GB in RAM.

Table 2. Description and dimension of parameters and optimization vectors

Vector name	Description	Dimension
X_{prod}	R_{LOX}, R_{LN2}	2
X_{opt}	X1, X2, X3, X4, XF	5
X_{fix}	Air feed molar fraction	3
	Temperature	17
	Purity	6
	Design Parameters	36
X_{exp}	Pressure and drop pressure	10
	Equipment efficiencies	11
	Valves drop pressure	9
	PINCH Temperature at HX3	1

Table 3. Operating variables and boundary values according to Figure 1

Name	Ratio	Boundary Upper	Boundary Lower	Definition and use in assessment
X1	F_2/F_{Air}	0.696	0.829	Refrigeration capacity
X2	F_4/F_3	0.290	1.000	Air fed ratio to HPC and LPC
X3	$\frac{F_{GN2}}{F_{Air}X_{N2,Air}}$	0.033	1.000	Waste nitrogen minimization
X4	F_{14}/F_{13}	0.000	0.980	Suitable heat duty in argon condenser
XF	$\frac{F_{EDM}-F_{feed}}{F_{EDM}}$	0.000	0.769	Feed loading variation

Table 4. Constraints used in the multi-objective optimization

Const.	Description	Condition	Equipment
1	Min. Pinch temperature, ΔT_P	$> 0\ K$	HX1
2	Min. Pinch temperature, ΔT_P	$> 0\ K$	HX2
3	Condenser excess heat duty, ΔQ_C	≤ 0 kW	Main. Cond.
4	Exergy destruction, $\dot{E}_D$	> 0 kW	Global process
5	Separator feasibility, L/G_{sep}	≥ 0.001	Sep. Argon

Results

Comparison of simulation results and data from the plant manual (EDM) and historical records resulted in absolute deviations below 12% in all variables. This indicates that the model describes reasonably well plant's performance and it can be confidently used for further optimization purposes. The summary of exergy destruction and the corresponding efficiencies of the main units are presented in Figure 3. The nitrogen vent accounts for nearly 50% of the plant capacity thus having the major impact in exergy destruction and efficiency, mainly affecting compression and expansion units. Overall efficiency is very low in comparison with similar plants (0.28, [5]), so optimization is heavily required.

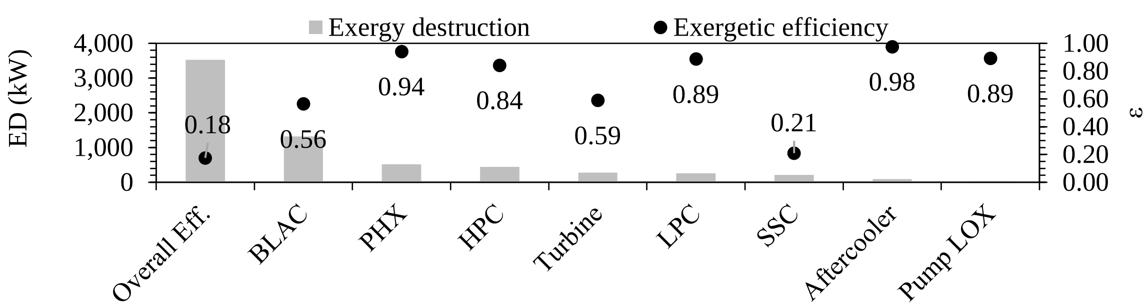

Figure 3. Exergy destruction ($\dot{E}_D$) and rational efficiency (ε) in major equipment of the air distillation plant

Results from optimization of the plant considering the variable monthly demand are presented in the Figure 4. Each pareto corresponds to the maximization of the objective function after 30 generations of the genetic algorithm with 40 individuals per generation (i.e. 14,400 evaluated cases), and it is unique for a given X_{prod}. As observed, the optimal pareto front for the recommended operating conditions of the plant manual (BOP) enables to obtain high argon recoveries but under intermediate or low exergy efficiencies indicating the primary goal of designers (i.e. high argon recovery for better economy). Optimization was mainly possible by changing feed flow of the plant (~ 20%) and reducing nitrogen vents. This indicates that the plant was overdesigned for the current demand but it is still operated at full capacity. So, there is need to adjust feed flows to increase exergy efficiency and to improve argon recovery. Under the feasible operating ranges of the plant for the different products demands, it is observed that exergy efficiency and argon recovery can change be up to 30% and 23%, respectively. These changes can derive in major improvements on the plant performance, mainly to reduce operating costs and to increase product sales. An important outcome of the optimization is that the plant can operate with a lower specific energy consumption (SPC). Comparing with the plant records it can be reduced up to a 35% under the different products demands.

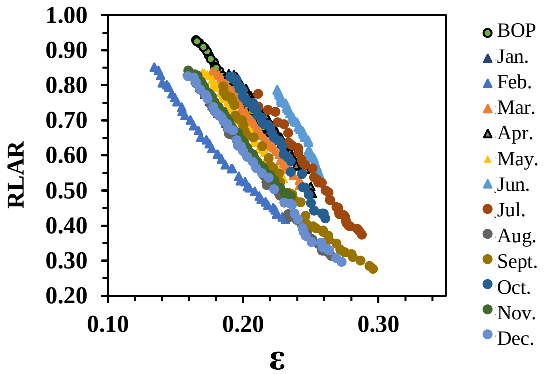

	X1	X2	X3	X4	XF	ε	R_{LAR}	SPC (kWh/Nm^3 O_2)	$\dot{E}_D$ (kW)
BOP	0.743	0.7955	1	0.0993	0.0642	0.1826	0.8403	0.83	3,361
Jan-19	0.7428	0.9113	0.2039	0.1393	0.3369	0.2221	0.5313	0.819	2,310
Feb-19	0.7530	0.9979	0.1824	0.0648	0.4760	0.2313	0.4187	0.780	1,828
Mar-19	0.7691	0.9834	0.3977	0.0000	0.3249	0.2419	0.5151	0.728	2,371
Apr-19	0.7742	0.9945	0.5611	0.1152	0.2761	0.2461	0.5602	0.707	2,547
May-19	0.7535	0.8619	0.3003	0.1232	0.3073	0.2298	0.5361	0.783	2,422
Jun-19	0.7798	0.8846	0.7353	0.0202	0.1782	0.2557	0.5557	0.678	2,891
Jul-19	0.8084	1.0000	0.8450	0.0312	0.3083	0.2711	0.4367	0.621	2,466
Aug-19	0.7897	0.6776	0.8378	0.2253	0.4461	0.2511	0.3615	0.692	1,974
Sep-19	0.7727	0.7070	0.7848	0.0000	0.3641	0.2520	0.3976	0.703	2,235
Oct-19	0.7701	0.8546	0.6815	0.1200	0.2823	0.2443	0.5092	0.721	2,525
Nov-19	0.7567	0.8756	0.3030	0.1525	0.3745	0.2356	0.4832	0.761	2,183
Dec-19	0.7763	0.9465	0.7665	0.0911	0.4620	0.2578	0.3510	0.685	1,888

Figure 4. Pareto front and optimal solutions under variable monthly demand of the studied air separation plant

It is important to point that the change in the operating flows of the CASU might have a great impact on the dynamic behavior of the system. Then, prior to the implementation of the optimal conditions for the corresponding variable demand, further studies are required to assess the impact of such changes in the performance of the cryogenic distillation columns, particularly in the separation efficiency and on their hydraulic behavior. However, it is expected that the columns would be resilient enough to withstand the proposed changes of the inlet air flowrate without major changes in the process performance. In this regard, as currently the plant operates under frequent shut-downs and start-ups due to tanks overloading or with large vents to release excess production, it is expected that the implementation of the recommended optimal operating conditions would help to reduce SPC and to increase exergy efficiency.

References

1. A. Smith, J. Klosek. Fuel Process Technol **70**: 115–34 (2001).
2. Y. A. Alsultanny, N. N. Al-Shammari. Eng. J. **18**:67–80 (2014).
3. G. Chen. Chem. Eng. Prog. **116** (6): 26-33 (2020).
4. Z. Khalel, A. Rabah, T. Barakat. ICASTOR J. Eng. **7**:135 – 147 (2014).
5. R. L. Cornelissen, G. G. Hirs. Energy Convers. Manag. **39**:1821–6 (1998)
6. X. B. Zhang, J. Y. Chen, L. Yao, Y. H. Huang, X. J. Zhang, L. M. Qiu. J. Zhejiang Univ. Sci. A **15**:309–22 (2014)
7. R. Agrawal, R. M. Thorogood. Gas Sep. Purif. 5:203–9 (1991)
8. Cornelissen, R. *Thermodynamics and sustainable development: The use of exergy analysis and the reduction of irreversibility.* Enschede: FEBODRUK BV, 1997.
9. S. N. Sapali, V. N. Raibhole. Lect. Notes Eng. Comput. Sci. **2**:621–5 (2013).
10. L. V. Van Der Ham. Energy Convers. Manag. **61**:31–42 (2012).
11. A. Ebrahimi, M. Meratizaman, H. A. Reyhani, O. Pourali, M. Amidpour. Energy **90**:1298–316. (2015)
12. M. H. Hamayun, N. Ramzan, M. Hussain, M. Faheem. Energies **13** (2020).
13. M. Mehrpooya, M. M. Sharifzadeh, M. A. Rosen. Energy **90**:2047–69 (2015).
14. C. A. Mora, A. Orjuela. Modeling, validation and exergy evaluation of a thermally-integrated industrial cryogenic air separation plant in Colombia. Chem. Eng. Res. Des. In revision.
15. M. J. Moran, H. N. Shapiro, S. Boettner, D. B. Daisie, M. B, Bailey. *Fundamentals of Engineering Thermodynamics*, 9th Edition. NY:Wiley. 2018.
16. F. Abdollahi-Demneh, M. A. Moosavian, M. R. Omidkhah, H. Bahmanyar. Energy **36**:5320–7 (2011).
17. Y. Zhu, S. Legg, C. D. Laird. Comput. Chem. Eng. 34:1377–84 (2010).
18. A. Briones-Ramírez, C. Gutiérrez-Antonio. Comput y Sist. **22**:1157–70 (2018).
19. K. Deb, A. Pratap, S. Agarwal, T. A. Meyarivan IEEE Trans Evol Comput **6**:182–97 (2002).
20. S. Lin. *NGPM — A NSGA-II Program in Matlab.* Coll Astronaut Northwest Polytech Univ China 2011.